Dioxygen Activation at Non-Heme Diiron Centers: Characterization of Intermediates in a Mutant Form of Toluene/*o*-Xylene Monooxygenase Hydroxylase

Leslie J. Murray,[†] Ricardo García-Serres,[‡] Sunil Naik,[‡] Boi Hanh Huynh,*,[‡] and Stephen J. Lippard*,[†]

Department of Chemistry, Massachusetts Institute of Technology, Cambridge, Massachusetts 02139, and Department of Physics, Emory University, Atlanta, Georgia 30322

Received April 20, 2006; E-mail: lippard@mit.edu; vhuynh@physics.emory.edu

Enzymes in the non-heme diiron super-family perform key biological functions ranging from radical generation for DNA biosynthesis to regio- and stereoselective oxidation of hydrocarbons at structurally similar active sites.[1] The features that determine the outcome of O_2 activation at these sites are unclear and are currently of great interest.

In the catalytic cycles of these enzymes, a diiron(II) center reacts with O_2 to generate reactive intermediates that have thus far been observed in only a few cases.[2,3] Among members of the sub-family of bacterial multicomponent monooxygenase (BMM) enzymes,[4] soluble methane monooxygenase is the only one for which intermediates have been observed. In this system, the reduced hydroxylase component, MMOH, reacts with O_2 to generate spectroscopically characterized diiron(III) and diiron(IV) intermediates.[3a,b] Both of these species can oxidize hydrocarbons,[3] which can enter the active site of MMOH via a string of hydrophobic pockets.[5] In contrast, a large substrate-access/product-egress channel is present in toluene/*o*-xylene monooxygenase hydroxylase (ToMOH), affording more exposed diiron sites.[6] We postulated that buffer components might quench the reactive intermediates in ToMOH and that mutations to block access to the diiron centers would facilitate the observation of intermediates. Following this strategy, we generated an I100W mutant in the α-subunit of the ToMOH by site-directed mutagenesis and discovered an oxygenated diiron intermediate that oxidizes the newly supplied W100 residue.

The reaction of the chemically reduced diiron(II) form of I100W ToMOH in the presence of the coupling protein, ToMOD, with O_2-saturated buffer was monitored by stopped-flow UV/visible spectroscopy. A transient species with an absorption band centered at 500 nm appeared with formation and decay rate constants $k_{form} = 0.804 \pm 0.001$ s^{-1} and $k_{decay} = 0.054 \pm 0.002$ s^{-1} and an extinction coefficient, ϵ_{500}, of $(1.5 \pm 0.2) \times 10^3$ M^{-1} cm^{-1} (Figure S1). On the basis of these optical properties, we tentatively assigned this species as a neutral tryptophan radical, W•.[7]

To investigate further the reaction of I100W ToMOH with O_2, rapid-freeze quench (RFQ) samples were prepared at various aging times and characterized by EPR and Mössbauer spectroscopy. A transient $g = 2.00$ EPR signal with fine structure (Figure 1) was observed, as expected for a W• species. The intensity of this signal maximized at ~3.5 s, consistent with the kinetics of formation of the putative W• radical from the UV/visible stopped-flow study. The EPR signal is easily saturated at 10 K and can be detected up to 50 K without any broadening, properties typical of an organic radical. When ^{57}Fe-enriched I100W was used in the reaction, however, hyperfine broadening was observed (Figure 1). This result unambiguously establishes that the diiron cluster contributes to this EPR signal. The observed hyperfine broadening is similar to that
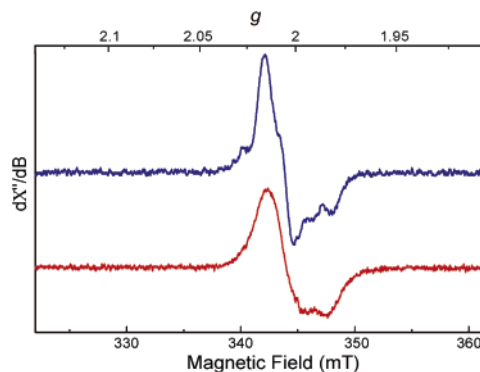

Figure 1. EPR spectra of the diiron(III,IV)−W• intermediate generated in the reaction of reduced ToMOH−I100W with O_2. The reaction was quenched at 4 s using natural abundant diiron(II) protein (blue) or at 3.5 s using ^{57}Fe-enriched protein (red).
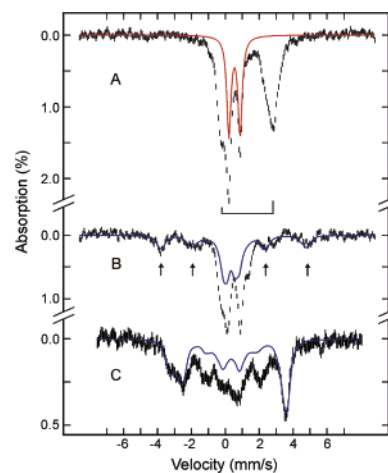

Figure 2. Mössbauer spectra of samples freeze-quenched at 70 ms (A) and 3.5 s (B and C) in the reaction of diiron(II) I100W ToMOH with O_2. The data were recorded at 4.2 K in a parallel applied field of 50 mT (A and B) or 8 T (C). For the spectra in B and C, the diiron(II) contributions (50% of the total Fe absorption) were removed from the raw data for clarity. Simulated spectra of the peroxo intermediate (A, red line) and of the **X**−Y• species in R2-W48F (B and C, blue lines) are superimposed and scaled to 30% of the total absorption of that sample. The bracket (A) indicates the diiron(II) protein. Raw data are denoted as vertical bars.

observed for the $g = 2.00$ EPR signals of the spin-coupled diiron-(III,IV) **X**-WH^{+}• in the ribonucleotide reductase R2 subunit (R2)[2c,g] and of **X**-Y• in the R2-W48F variant.[2h] The optical absorption and EPR spectral data therefore suggest a spin-coupled intermediate comprising W• and a paramagnetic diiron cluster. Mössbauer data (Figure 2) confirmed the spin-coupled nature of this intermediate

† Massachusetts Institute of Technology.
‡ Emory University.

and revealed the oxidation state of the paramagnetic diiron center to be mixed-valent diiron(III,IV).

Figure 2B displays the 4.2 K Mössbauer spectrum of the 3.5 s RFQ sample recorded with a 50 mT magnetic field applied parallel to the γ-beam. A paramagnetic spectral component with features (arrows) similar to those of the diiron(III,IV) intermediate, **X**, in R2[2g,h] was observed. Analysis of the spectrum indicates that this component accounts for $15 \pm 2\%$ of the total Fe absorption. The spectrum of this sample recorded with a strong applied field of 8 T (Figure 2C) showed a 2-fold increase in the intensity of the paramagnetic component to $30 \pm 3\%$ of total Fe absorption. This field-dependent increase of the paramagnetic absorption indicates that the $S = 1/2$ diiron(III,IV) cluster is weakly spin-coupled to a nearby $S = 1/2$ paramagnet.[2h] For a weakly coupled system ($J <$ 1 cm^{-1}) in a weak applied field of 50 mT, the energy separations of the four electronic levels are small, whereas in a strong applied field of 8 T, the Zeeman interaction increases the energy separations between these levels. At 4.2 K and 50 mT, all four levels are nearly equally populated, and the spectrum contains two equal-intensity components: a paramagnetic component (two $M_S = \pm 1$ sublevels of the triplet state) superposed on a "diamagnetic" component (the singlet state and the $M_S = 0$ sublevel of the triplet state). In contrast, at 4.2 K and 8 T, only the lowest $M_S = -1$ sublevel is populated and the diamagnetic component disappears, doubling the intensity of the paramagnetic component.[2h] We compared a simulated spectrum of the X$-$Y$^{\bullet}$ species in R2-W48F (Figure 2) to the spectrum of the 3.5 s sample, and the agreement is remarkable and consistent with our assignment. The observed discrepancy in the central region of the spectrum indicates the presence of another intermediate (vide infra) and a diiron(III) product; in addition, the Mössbauer parameters for the I100W diiron(III,IV) may be slightly different than those of **X** in R2-W48F.

Time-dependent EPR experiments indicate that the diiron(II) g = 16 signal decays more rapidly ($\sim$60 s^{-1}) than the formation rate of the diiron(III,IV)$-$W$^{\bullet}$ g = 2 signal (data not shown). An EPR-silent precursor to the diiron(III,IV)$-$W$^{\bullet}$ species therefore must exist, the concentration of which would maximize at a reaction time of $\sim$100 ms. Consistent with this conclusion, the Mössbauer spectrum of a sample quenched at 70 ms (Figure 2A) shows a sharp quadrupole doublet accounting for approximately 30% of the total Fe absorption, as well as the broad quadrupole doublet of the initial diiron(II) protein. The parameters of the sharp quadrupole doublet ($\delta = 0.54 \pm 0.02$ mm/s and $\Delta E_Q = 0.66 \pm 0.03$ mm/s) are typical of high-spin Fe^{III} species. Spectra recorded with strong applied fields and the EPR data indicate that this doublet arises from an antiferromagnetically coupled diiron(III) cluster. In the 3.5 s sample, the intensity of this doublet is diminished substantially and accounts for less than 7% of the Fe absorption, establishing that this diiron(III) intermediate decays during formation of the spin-coupled diiron(III,IV)$-$W$^{\bullet}$ species. This diiron(III) species is the first observable intermediate after reaction with O$_2$, and on the basis of the work with other non-heme diiron proteins,[2] we tentatively assign this species as a peroxodiiron(III) unit. The Mössbauer parameters for this species in I100W ToMOH, however, differ from those reported for the peroxodiiron(III) intermediates in other carboxylate-bridged diiron proteins, for which $\delta > 0.6$ mm/s and $\Delta E_Q > 1.00$ mm/s.[8] Furthermore, the peroxo species in these proteins exhibit optical absorptions with λ_{max} greater than 650 nm,[2d–g] and no such features are observed for I100W ToMOH. Peroxodiiron(III) synthetic complexes with a planar μ-1,2-peroxo coordination mode and a second bridging ligand[9] have δ and ΔE_Q values similar to those reported here for the putative peroxodiiron(III) intermediate. The mechanism by which the diiron(III,IV) center and W$^{\bullet}$ radical form

in I100W ToMOH may be similar to that proposed for the generation of **X** and Y$^{\bullet}$ in R2.[2h] Preliminary evidence indicates that decay of the diiron(III,IV) and W$^{\bullet}$ species may proceed via hydroxylation of W100, the closest distance from a carbon atom in the tryptophan side chain to a bridging hydroxide in the {Fe$_2$(μ-OH)$_2$}$^{4+}$ core being $\sim$6.5 Å (unpublished results).

The detection of an early transient for I100W ToMOH with Mössbauer parameters atypical of those for peroxodiiron(III) species and no obvious visible absorption band led us to examine the time-dependent Mössbauer spectra of the reaction of the wild-type enzyme with O$_2$. The results indicate unambiguously the accumulation of a transient with a spectrum identical to that observed for the diiron(III) intermediate in the I100W ToMOH variant (unpublished results). Detailed spectroscopic investigations of this intermediate are in progress. Peroxo[3c,10] and hydroperoxo[11] species are proposed to be reactive intermediates in metalloenzymes, and this putative peroxo adduct may be the active oxidant for aromatic hydroxylation in the ToMO systems.

Supporting Information Available: Experimental details for sample preparation, stopped-flow UV/visible data, and EPR acquisition parameters. This material is available free of charge via the Internet at http://pubs.acs.org.

References

(1) Kurtz, D. M., Jr. *J. Biol. Inorg. Chem.* **1997**, *2*, 159–167.

(2) (a) Lee, S.-K.; Fox, B. G.; Froland, W. A.; Lipscomb, J. D.; Münck, E. *J. Am. Chem. Soc.* **1993**, *115*, 6450–6451 (b) Liu, K. E.; Wang, D.; Huynh, B. H.; Edmonsdon, D. E.; Salifoglou, A.; Lippard, S. J. *J. Am. Chem. Soc.* **1994**, *116*, 7465–7466. (c) Burdi, D.; Willems, J.-P.; Riggs-Gelasco, P.; Antholine, W. E.; Stubbe, J.; Hoffman, B. M. *J. Am. Chem. Soc.* **1998**, *120*, 12910–12919. (d) Moënne-Loccoz, P.; Baldwin, J.; Ley, B. A.; Loehr, T. M.; Bollinger, J. M., Jr. *Biochemistry* **1998**, *37*, 14659–14663. (e) Pereira, A. S.; Small, W.; Krebs, C.; Tavares, P.; Edmondson, D. E.; Theil, E. C.; Huynh, B. H. *Biochemistry* **1998**, *37*, 9871–9876. (f) Broadwater, J. A.; Ai, J.; Loehr, T. M.; Sanders-Loehr, J.; Fox, B. G. *Biochemistry* **1998**, *37*, 14664–14671. (g) Baldwin, J.; Krebs, C.; Ley, B. A.; Edmondson, D. E.; Huynh, B. H.; Bollinger, J. M., Jr. *J. Am. Chem. Soc.* **2000**, *122*, 12195–12206. (h) Krebs, C.; Chen, S.; Baldwin, J.; Ley, B. A.; Patel, U.; Edmonsdon, D. E.; Huynh, B. H.; Bollinger, J. M., Jr. *J. Am. Chem. Soc.* **2000**, *122*, 12207–12219.

(3) (a) Nesheim, J. C.; Lipscomb, J. D. *Biochemistry* **1996**, *35*, 10240–10247. (b) Valentine, A. M.; Stahl, S. S.; Lippard, S. J. *J. Am. Chem. Soc.* **1999**, *121*, 3876–3887. (c) Beauvais, L. G.; Lippard, S. J. *J. Am. Chem. Soc.* **2005**, *127*, 7370–7378.

(4) Leahy, J. G.; Batchelor, P. J.; Morcomb, S. M. *FEMS Micro. Rev.* **2003**, *27*, 449–479.

(5) (a) Rosenzweig, A. C.; Brandstetter, H.; Whittington, D. A.; Nordlund, P.; Lippard, S. J.; Frederick, C. A. *Proteins* **1997**, *29*, 141–152. (b) Whittington, D. A.; Rosenzweig, A. C.; Frederick, C. A.; Lippard, S. J. *Biochemistry* **2001**, *40*, 3476–3482.

(6) Sazinsky, M. H.; Bard, J.; Di Donato, A.; Lippard, S. J. *J. Biol. Chem.* **2004**, *279*, 30600–30610.

(7) Aubert, C.; Vos, M. H.; Mathis, P.; Eker, A. P. M.; Brettel, K. *Nature* **2000**, *405*, 586–590.

(8) Merkx, M.; Kopp, D. A.; Sazinsky, M. H.; Blazyk, J. L.; Müller, J.; Lippard, S. J. *Angew. Chem., Int. Ed.* **2001**, *40*, 2782–2807.

(9) (a) Menage, S.; Brennan, B. A.; Juarez-Garcia, C.; Münck, E.; Que, L., Jr. *J. Am. Chem. Soc.* **1990**, *112*, 6423–6425. (b) Dong, Y.; Yan, S.; Young, V. G., Jr.; Que, L., Jr. *Angew. Chem., Int. Ed. Engl.* **1996**, *35*, 618–620. (c) Zhang, X.; Furutachi, H.; Fujinami, S.; Nagatomo, S.; Maeda, Y.; Watanabe, Y.; Kitagawa, T.; Suzuki, M. *J. Am. Chem. Soc.* **2005**, *127*, 826–827.

(10) (a) Decker, H.; Dillinger, R.; Tuczek, F. *Angew. Chem., Int. Ed.* **2000**, *39*, 1591–1595. (b) Baldwin, J.; Voegtli, W. C.; Khidekel, N.; Moënne-Loccoz, P.; Krebs, C.; Pereira, A. S.; Ley, B. A.; Huynh, B. H.; Loehr, T. M.; Riggs-Gelasco, P. J.; Rosenzweig, A. C.; Bollinger, J. M., Jr. *J. Am. Chem. Soc.* **2001**, *123*, 7017–7030. (c) Yamazaki, S.-i.; Morioka, C.; Itoh, S. *Biochemistry* **2004**, *43*, 11546–11553.

(11) (a) Vatsis, K. P.; Coon, M. J. *Arch. Biochem. Biophys.* **2002**, *397*, 119–129. (b) Jin, S.; Bryson, T. A.; Dawson, J. H. *J. Biol. Inorg. Chem.* **2004**, *9*, 644–653. (c) Nam, W.; Ryu, Y. O.; Song, W. J. *J. Biol. Inorg. Chem.* **2004**, *9*, 654–660.

JA062762L